Fabrication of large-area concave microlens array on silicon by femtosecond laser micromachining

Zefang Deng, Qing Yang, Feng Chen,* Xiangwei Meng, Hao Bian, Jiale Yong, Chao Shan, and Xun Hou

State Key Laboratory for Manufacturing System Engineering and Key Laboratory of Photonics Technology for Information of Shaanxi Province, School of Electronics and Information Engineering, Xi'an Jiaotong University, Xi'an 710049, China

**Corresponding author: chenfeng@mail.xjtu.edu.cn*

Received December 3, 2014; revised March 23, 2015; accepted March 30, 2015;
posted March 31, 2015 (Doc. ID 228756); published April 20, 2015

In this Letter, a novel fabrication of large-area concave microlens array (MLA) on silicon is demonstrated by combination of high-speed laser scanning, which would result in single femtosecond laser pulse ablation on surface of silicon, and subsequent wet etching. Microscale concave microlenses with tunable dimensions and accessional aspherical profile are readily obtained on the 1 cm × 1 cm silicon film, which are useful as optical elements for infrared (IR) applications. The aperture diameter and height of the microlens were characterized and the results reveal that they are both proportional to the laser scanning speed. Moreover, the optical property of high-performance silicon MLAs as a reflective homogenizer was investigated for the visible wavelength, and it can be easily extended to IR light. © 2015 Optical Society of America

OCIS codes: (160.6030) Silica; (230.0230) Optical devices; (230.1360) Beam splitters; (230.4040) Mirrors; (350.3390) Laser materials processing.

http://dx.doi.org/10.1364/OL.40.001928

Compound eyes in nature, which generally refer to structures comprising of thousands of integrated micro-optical units, have attracted great interest in diverse fields of micro-optics due to their intriguing capabilities for large field-of-view (FOV) imaging with minimized volume and high sensitivity [1–3]. Among these, there are some special insects (e.g., Dung beetle, ant, and nocturnal hawkmoths) that they possess infrared (IR)-sensitive compound eyes [4,5], which exhibit potential application in IR wide FOV imaging, detection, and beam shaping [6,7]. However, current biomimetic compound eyes are mostly based on visible light, and various methods have been reported to fabricate compound-eye-like structures under visible light, such as laser direct writing, reconfigurable microtemplating, and surface wrinkling [8–11]. In contrast, there are few studies in infrared compound-eye-like micro-optical elements. Especially, efficient fabrication of large-area IR micro-optical elements with high fill ratio is still challenging.

In the past decades, femtosecond laser has been demonstrated as a promising tool for fabricating microstructures in transparent materials, such as silica glass [12–14]. In such technology, the silica glass is first irradiated by focused femtosecond laser and modification material with higher chemical etching rate can be locally formed [14], owing to multiphoton absorption, avalanche ionization, and subsequent formation of a microexplosion [15]. Then, the modification area is promptly removed by wet chemical etching.

Silicon (Si) is one of important fundamental materials because of its broad mid-IR transparency and easy integration into sophisticated silicon microelectronics device. Meanwhile, the focused femtosecond laser irradiation would generate induced stress, structural changes, and amorphization in the silicon, resulting in local chemical activity enhancement [16–18]. In this Letter, large-area concave all-silicon microlens array (MLA) was rapidly fabricated by single-pulsed femtosecond laser wet etching (sp-FLWE) process, which is a combination of femtosecond (fs) laser high-speed scanning irradiation and subsequent wet etching. The profiles of fabricated microlenses were parabolic, and about 3 million microlenses could be fabricated within 1 h. Besides, MLAs with different dimensions were acquired by adjusting the laser scanning speed. It was shown that the height and aperture diameter of the fabricated microlenses were both approximately proportional to the laser scanning speed. Hence, the microlens morphology could be easily controlled. The fill factor of the MLA reached 99%, and its optical property as a reflected homogenizer was characterized by a He–Ne laser.

Figure 1(a) shows a schematic diagram of the experimental configuration. The laser was generated by the regeneratively amplified Ti:sapphire laser system (Coherent Libra-usp-he, pulse duration 50 fs, central wavelength 800 nm, repetition rate 1 kHz). The laser output beam was focused by a 0.50 NA, 50× objective lens (Nikon) onto the surface of 0.4 mm thick silicon wafer with ⟨100⟩ orientation. The laser focal spot size on the substrate was about

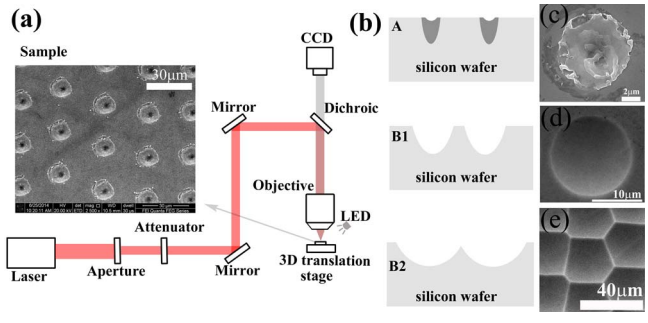

Fig. 1. (a) Experimental setup for laser scanning process. Inset, array of pulse-irradiated craters. (b) Process sequence for fabricating close-packed microlenses over a silicon wafer. Step A, laser induced material modification; Step B1, forming concave microstructure by chemical etching; Step B2, etching until adjacent concave microstructures squeeze with each other. (c) SEM image of laser-modification zone. (d) SEM image of circular concave microstructures. (e) SEM images of irregular concave microstructures.

 © 2015 Optical Society of America

2 μm. The silicon specimen was mounted horizontally on a three-axis translation stage (M-505.2DG, Physik Instrumente), which has a step size of 100 nm. A white LED illuminated microscope was incorporated for observing the sample. The surface of the silicon sample was imaged onto the CCD, thus one could accurately determine the horizontality of the sample by translating it in a direction perpendicular to the laser beam.

The fabrication process for the concave silicon microstructures is shown in Fig. 1(b). The first step was that the focused laser irradiated on surface of the silicon substrates to induce local material modification. The energy of the incident laser pulse, which could be controlled by the variable neutral density filter [Fig. 1(a)], was set to 8 μJ (with an average irradiance of 1.28×10^{15} W/cm^2 [19]). By translating the wafers line-by-line using the stage at a high speed, an array of laser induced craters was generated. They were arranged in quasi-periodic with a period of s micrometers, and the period could be controlled by computer programming. Moreover, the interspacing between adjacent craters, s micrometers, was proportional to the stage speed ($s \times 10^3$ μm/s) as the pulse repetition rate maintains a constant.

During the next step, the processed wafers were dipped into isotropic etching solution with ultrasonic water bath (55 kHz) to form concave microstructures. A solution consisting of hydrofluoric acid (HF), nitric acid (HNO_3), and acetic acid (CH_3COOH), i.e., HNA, with a specific formulation, was utilized as the etching solution. In general, the silicon etching in the HNA system could be summarized as follows

$$3Si + 4HNO_3 + 8HF \rightarrow 3H_2SiF_6 + 4NO + 8H_2O.$$

In the reaction, HNO_3 acted as an oxidizing agent to form oxide, which would be subsequently dissolved by HF; and CH_3COOH was considered to be a diluent. Hence, the etching rate and acid-etched surface roughness of the silicon could be influenced by the composition of the HNA [20]. In our work, the HNA composition of HF:HNO_3:CH_3COOH = 6:10:9 by volume was utilized after repeatedly optimizing. The mass fractions of HF, HNO_3, and CH_3COOH were 40%, 60%, and ≥99.5%, respectively. In the initial process of the etching [Step B1 in Fig. 1(b)], circular concave microstructures [Fig. 1(d)] would be created in the laser-irradiated zone and evenly expanded until the laser-modified materials had been etched out [Fig. 1(c)]. Sequentially, the samples were etched until the concave microstructures squeezed each other to form a close-packed array [Fig. 1(e)], as in Step B2 shown in Fig. 1(b).

To characterize the surface morphology of the fabricated microstructures, a field-emission (FE) scanning electron microscope (SEM; FEOLJSM-7000F) was employed, and the 3D morphology data were quantified by a laser scanning confocal microscope (LCSM; Olympus LEXT OLS4000). Figures 2(a) and 2(d), respectively, show the concave microstructure arrays with different aperture diameters fabricated by the sp-FLWE with a laser scanning speed of 20 and 30 mm/s. The microstructures, covering the total area of the silicon wafer with the dimensions of 10 mm × 10 mm, were quasi-periodic arranged and irregular-shaped microlenses. Second,

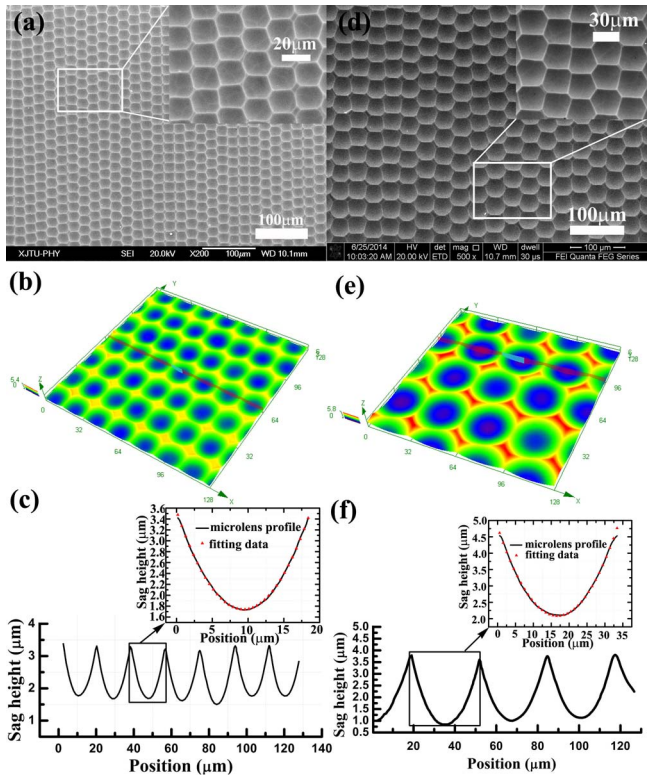

Fig. 2. (a–c) and (d–f) are the SEM image, 3D morphology, and cross sectional profiles of the concave microstructures with an average diameter of 20 and 30 μm, respectively. Insets in (c) and (f) are the enlarged view of the data in the box and its profile fitting.

the SEM images in Figs. 2(a) and 2(d) show the magnified images of the boxed areas, in which close-packed microstructures without gaps could be observed. The fill factor of the concave microstructures reached 99%.

The 3D and 2D profiles of the microlenses are shown in Figs. 2(b) and 2(c), and 2(e) and 2(f), respectively. To demonstrate the uniformity of the fabricated microlenses, different regions of the silicon wafer were measured and the data were treated with statistical processing and analysis. Consequently, the average aperture diameters and sag heights of a microlens are 19.5 and 1.5 μm, and 32.8 and 2.5 μm, respectively, and the standard deviations are 1.6 and 0.2 μm, and 2.7 and 0.4 μm, respectively. Although the deviations increased with the growth of the aperture diameter, the deviations might be reduced by stabilizing the laser output power. Moreover, according to the measurements and theoretical fitting data, as shown in Figs. 2(e) and 2(f), the microlenses have a parabolic shape, where the radius of the curvature at the vertex are about 97.3 and 206.6 μm, respectively, and the root-mean square (RMS) deviations are both less than 60 nm.

Figure 3(a) shows the cross section of the sag surfaces of the fabricated microlenses for a varying laser scanning speed. With data fitting between the sag surface profiles and the standard conic section curve, such as spherical, elliptical, and parabolic, we found that a parabolic surface lead to the smallest RMS deviation (less than 60 nm). Hence, it is reasonable to regard the sag surface of the fabricated microlenses as parabolic. Moreover, the

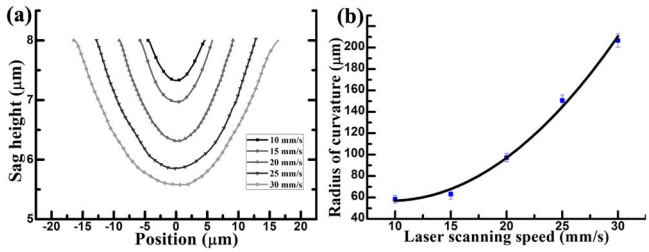

Fig. 3. (a) Cross sectional profiles of fabricated microlenses with different laser scanning speeds. (b) Evolution of the radius of curvature at the vertex of the fabricated microlenses versus the laser scanning speed.

radius of the curvature (ROC) at the vertex of the fabricated microlenses could be calculated, which were 58.4, 63.2, 97.3, 150.6, and 206.6 μm, respectively. It is clear that the ROC increase with the laser scanning speed, as shown in Fig. 3(b).

The sag heights and aperture diameters of the fabricated microlenses were measured using LCSM and are plotted in Fig. 4(a) as a function of the laser scanning speed. The data were measured from different areas of the silicon wafer. It is noted that the height and aperture diameter of the fabricated microlenses are both approximately proportional to the laser scanning speed. However, it is important to note that the aperture diameters ranging from 10 to 30 μm are available in our experimental condition, owing to the maximum speed limitation of the translation stage. Figure 4(b) shows the influence of the different pulse energies on dimensions of the fabricated microlenses. The laser scanning speed was set as 30 mm/s, and the etching time was 6 min.

Based on the previous results and analysis, we could note that the fabricated MLAs have series of unique specialized characteristics. First, the nonperiodic distribution of the arrays would effectively suppress interference pattern especially in the application of highly coherent light. Second, the high filling ratio of the MLA would not only enhance the light utilization efficiency but reduce the noise of the emergent light.

The optical performance of the reflected MLA was also demonstrated with an optical system, as shown in Fig. 5(a). The optical system was based on a He–Ne laser with the wavelength of 632 nm. The output beam of the He–Ne laser was circular, and its diameter was 0.6 mm. In order to cover the central part of MLAs, the laser beam was expanded to about 3 mm with a couple of lenses (L1 and L2). The fabricated reflected-diffuse was placed at

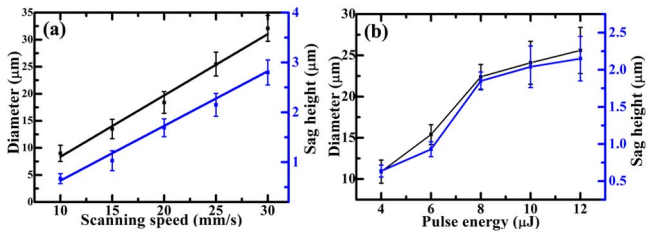

Fig. 4. (a) Effects of laser scanning speed on the fabricated microlens shape. (b) Change of the aperture diameter (square markers) and the sag height (triangle markers) with the pulse energy.

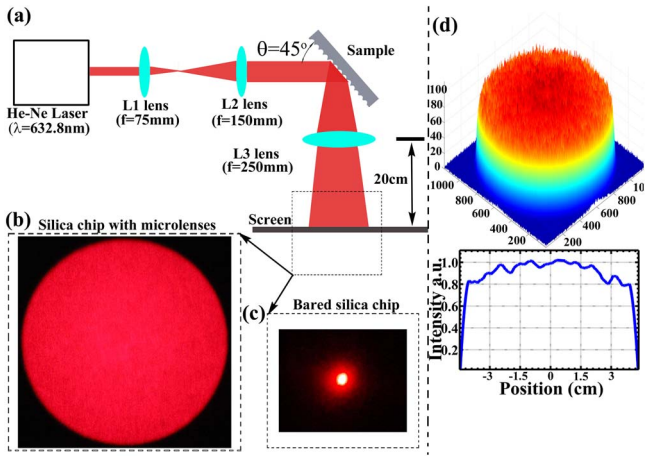

Fig. 5. (a) Optical system used for measuring the refracted illumination distribution. (b) Illumination distribution of MLAs. (c) Illumination distribution of bare silica chip. (d) 3D intensity distribution and cross sectional profile of the homogenized beam with MLAs.

the angle of 45° against the incident laser, which was perpendicular to the emergent light. The MLA divided the incoming beam into a number of beamlets by its multi-aperture elements. Sequentially, the beamlets overlapped onto a piece of print paper with a help of a imaging lens (L3, $f = 250$ mm) and were imaged by a color CCD camera. The print paper was served as the detector screen and be placed 200 mm away from L3. Figure 5(b) shows the homogeneous illumination of the reflected MLAs with average diameter of 20 μm. Meanwhile, a bare silica chip was replaced the reflected diffuser, and its illumination pattern was measured, as shown in Fig. 5(c). Although the diameter of the detected light beam expanded to about 5 mm, it remained a typical Gaussian distribution. Moreover, a digital manipulation was utilized to analyze the illumination distribution of the laser beam that was detected. Figure 5(d) shows the intensity distribution of the homogenized beam of the reflected diffuser. After shaped by the fabricated diffuser, the output beams are nearly flat top. The size of the homogeneous beam is about 9 cm.

In summary, large-area multi-aperture structures consisting of concave microlenses were rapidly fabricated on silicon using a sp-FLWE technique. The technique is based on fs laser high-speed scanning irradiation and the subsequent wet etching. Aspherical microlenses with diameters ranging from 10 to 30 μm could be created on the 1 cm × 1 cm silicon wafer. It was also experimentally demonstrated that the diameter and the height of the concave microlenses could be controlled by the laser scanning speed. Serving the fabricated concave MLAs as a mold, the convex MLAs structures can be replicated on other materials, such as PMMA, by hot-embossing technology. Moreover, these concave MLAs have been demonstrated as a reflected homogenizer for visible wavelengths. Because of its transparency in the IR, these concave silicon MLAs can be simply extended to IR light for homogenization.

This work was supported by the National Science Foundation of China under Grant Nos. 51335008,

61275008, 61475124, and 61405154, and the special-funded Program on National Key Scientific Instruments and Equipment Development of China under Grant No. 2012YQ12004706.

References

1. L. P. Lee and R. Szema, Science **310**, 1148 (2005).
2. J. Kim, K. H. Feong, and L. P. Lee, Opt. Lett. **30**, 5 (2005).
3. A. Brückner, J. D. A. Brückner, J. Duparré, P. Dannberg, A. Bräuer, and A. Tünnermann, Opt. Express **15**, 11922 (2007).
4. P. McIntyre and S. Cavney, J. Comp. Physiol. A **183**, 45 (1998).
5. A. Kelber, A. Balkenius, and E. J. Warrant, Nature **419**, 922 (2005).
6. M. Tormen, A. Carpentiero, E. Ferrari, D. Cojoc, and E. D. Fabrizio, Nanotechnology **18**, 385301 (2007).
7. C. C. Huang, X. D. Wu, H. W. Liu, B. Aldalali, J. A. Rogers, and H. R. Jiang, Small **10**, 3050 (2014).
8. D. Radtke, J. Duparré, U. D. Zeitner, and A. Tünnermann, Opt. Express **15**, 3067 (2007).
9. D. Wu, J. N. Wang, L. G. Niu, X. L. Zhang, S. Z. Wu, Q. D. Chen, L. P. Lee, and H. B. Sun, Adv. Opt. Mater. **2**, 751 (2014).
10. K. H. Jeong, J. Kim, and L. P. Lee, Science **312**, 557 (2006).
11. E. P. Chan and A. J. Crosby, Adv. Mater. **18**, 3238 (2006).
12. S. He, F. Chen, K. Liu, Q. Yang, H. Liu, H. Bian, X. Meng, C. Shan, J. Si, and Y. Zhao, Opt. Lett. **37**, 3825 (2012).
13. F. Chen, H. W. Liu, Q. Yang, X. H. Wang, C. Hou, H. Bian, W. W. Liang, J. H. Si, and X. Hou, Opt. Express **18**, 20334 (2010).
14. A. Marcinkevičius, S. Juodkazis, M. Watanabe, M. Miwa, S. Matsuo, and H. Misawa, Opt. Lett. **26**, 277 (2001).
15. R. R. Gattass and E. Mazur, Nat. Photonics **2**, 219 (2008).
16. V. Domnich, Y. Gogotsi, and S. Dub, Appl. Phys. Lett. **76**, 2214 (2000).
17. A. Kiani, K. Venkatakrishnan, and B. Tan, Opt. Express **17**, 16518 (2009).
18. X. Zhao and Y. C. Shin, J. Phys. D **46**, 335501 (2013).
19. R. Buividas, S. Rekštytė, M. Malinauskas, and S. Juodkazis, Opt. Mater. Express **3**, 1674 (2013).
20. A. A. Hamzah, N. A. Aziz, B. Y. Majlis, J. Yunas, C. F. Dee, and B. Bais, J. Micromech. Microeng. **22**, 095017 (2012).